ELSEVIER

ICS

# Construction of a probabilistic atlas for automated liver segmentation in non-contrast torso CT images

X. Zhou[a,*], T. Kitagawa[a], K. Okuo[a], T. Hara[a], H. Fujita[a], R. Yokoyama[b], M. Kanematsu[b], H. Hoshi[b]

[a]Department of Intelligent Image Information, Division of Regeneration and Advanced Medical Sciences, Graduate School of Medicine, Gifu University, Gifu, Japan
[b]Department of Radiology, Gifu University School of Medicine and University Hospital, Gifu, Japan

**Abstract.** In this paper, we proposed a method to generate a probabilistic atlas of liver and use it for liver region segmentation from non-contrast torso CT images. The atlas was defined by two kinds of probability: liver location and its density (CT number). We developed a method to normalize the liver location in different patient cases by deforming the pre-segmented diaphragm and bone to a standard position and to generate a normalized likelihood image to present probability of liver location in torso CT image by projecting a large number of liver regions into a 3-D space. A Gaussian window function with dynamic parameter estimations was used to calculate the probability of liver density. 80 patient cases of non-contrast CT images with the pre-segmented liver regions were used for performance evaluation. We repeated the atlas generation and atlas-based segmentation of liver region based on non-contrast torso CT images using a leave-one-out method. The mean value of the coincidence ratio between the pre-segmented liver and atlas-based segmentation result was found to be 84%. The validation and usefulness of our atlas construction method were proved. © 2005 CARS & Elsevier B.V. All rights reserved.

## 1. Introduction

The remarkable progresses of multi-slice CT technology enable radiologists to scan a larger volume of human body in a shorter scan time with a higher isotropic spatial resolution in one-time CT imaging. The computer-aided diagnosis (CAD) system is

* Corresponding author. Tel./fax: +81 58 230 6510.
  *E-mail address:* zxr@fjt.info.gifu-u.ac.jp (X. Zhou).

expected to increase the lesion detection accuracy of radiologist and decrease the interpretation burden. Liver is one of the most important diagnosis target organs of the CAD system. Lesion detection and surgery planning of liver always require the CAD system to extract the liver region firstly from CT images. However, without any prior information, the traditional image processing methods cannot provide a reliable extraction of liver region automatically from non-contrast CT images. The atlas-based segmentation can be expected to solve this problem. Park et al. proposed a method for abdominal probabilistic atlas construction [1] and some further approaches were also reported [2,3]. However, how to map the anatomical structures between different CT images automatically and precisely could not be solved completely in [1–3]. Spatial registration for an organ region in different CT images is very important not only for atlas construction but also for atlas-based segmentation. In this paper, we proposed a new method to normalize the anatomical location of liver based on the diaphragm warping and construct a probabilistic atlas with high precision for liver in torso CT images. Finally, we also showed a fully-automatic approach to segment liver region from non-contrast torso CT images based on probabilistic atlas.

## 2. Methods

### 2.1. Probability of liver region

We define the $P(A)$ as the probability of each voxel that belongs to liver region in a CT image, and $P(B)$ as the probability of liver location in the spatial anatomical structure of human torso, and $P(C|B)$ as the density (CT number) distribution of liver region in a CT image. Using the above definitions, we can get the following equation.

$$P(A) = P(B \cap C) = P(B) \times P(C|B) \tag{1}$$

The probability $P(A)$ is regarded as the "liver probabilistic atlas" which can be calculated by $P(B)$ [probability of the anatomical location of liver region in human torso] and $P(C|B)$ [density histogram (probability) of the liver region in a CT image]. This research tries to develop the methods to estimate the $P(B)$ and $P(C|B)$ and generate the probabilistic atlas $P(A)$ for liver segmentation.

### 2.2. Construction of liver probabilistic atlas

We investigated a method to estimate the probability $P(B)$ based on the anatomical structure of human body. The spatial relations between liver, bone structure, and diaphragm were used for the estimation (Fig. 1). Our method normalized the liver position, size, and shape by adjusting the cross-sectional area of bone frame to a standard and warping the diaphragm to a plane based on a thin-plate spline method [4] firstly (refer to Fig. 1(c)), and then create a normalized likelihood image of liver by projecting a lot of pre-segmented liver regions into a 3-D space (refer to Fig. 1(d)). For an unknown CT image, we can extract the bone and diaphragm [5,6] firstly and warp the normalized likelihood image (Fig. 1(d)) inversely to estimate the $P(B)$ of the liver location in inputted CT image.

After the $P(B)$ estimation, we proposed a method to estimate the $P(C|B)$ that can be considered as the density distribution inside of the liver regions. We used a
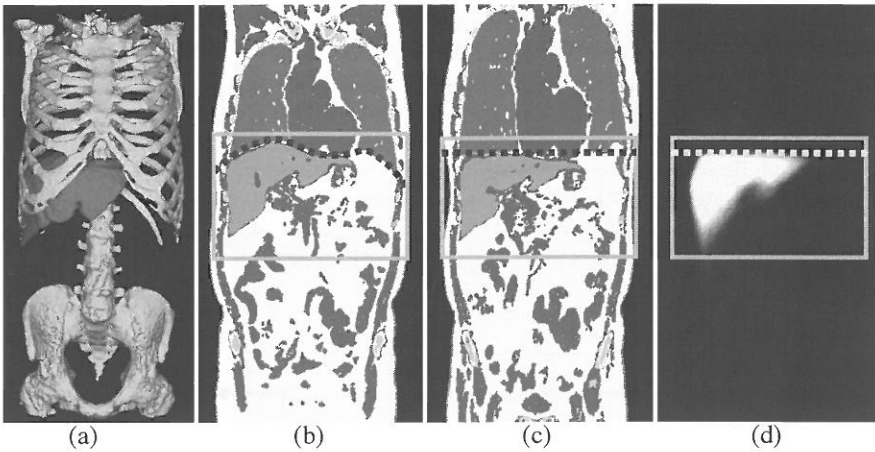
Fig. 1. The probability estimation for liver location. (a) Pre-segmented liver and bone. (b) Spatial relations between liver, bone, and diaphragm (dotted line). (c) Normalizing liver position and shape by deforming the diaphragm and bone to a standard position (rectangle). (d) Spatial voting to generate a normalized likelihood image to show the probability of liver location using 80 patient cases of CT.

Gaussian model to approximate the density distribution of liver by the following equation.

$$p(y_i | i \in \text{Liver}) = \frac{1}{\sqrt{2\pi\sigma^2}} \exp\left(\frac{-(y_i - \mu)^2}{2\sigma^2}\right) \tag{2}$$

The Gaussian parameters can be estimated by observing the density histogram of the region that each voxel $i$ should satisfy the condition $[P_i(B) > 0]$. We selected the CT number which was the maximum peak in the histogram as the mean value $\mu$ and decided a Gaussian distribution $N(\mu, \sigma)$ which had the same FWHM (full width half maximum) with the observed density histogram. Then, we calculated the $P(C|B)$ from the CT images by a probability transformation using the $N(\mu, \sigma)$ as a characteristic curve (Fig. 2). A likelihood image (Fig. 2(c)) was generated to show the probability $P(C|B)$ which indicates the probability of liver on CT numbers.

The probability $P(A)$ for a CT image can be obtained simply by a multiplication of $P(B)$ and $P(C|B)$. In fact, we generated a total likelihood image of liver as the probabilistic atlas by an image multiplication (see following section).

## 2.3. Atlas-based liver region segmentation

Using the constructed probabilistic atlas, we developed a procedure to segment a liver region from torso CT images. This procedure includes 5 processing steps. We describe each processing step as following sentences and shown schematically in Fig. 3. (1) The bone region is extracted using a gray-level thresholding method [5] and the diaphragm is identified based on the shape of air regions inside the lungs [6]. (2) Using the bone and diaphragm (Fig. 3(b)), the normalized likelihood image of liver location (Fig. 3(c)) is warped and a special likelihood image (Fig. 3(d)) that shows the probability $P(B)$ of liver location for inputted CT images is generated. (3) Based on the region that satisfied $P(B) > 0$, the density probability $P(C|B)$ (Fig. 3(e)) is estimated using a transformation
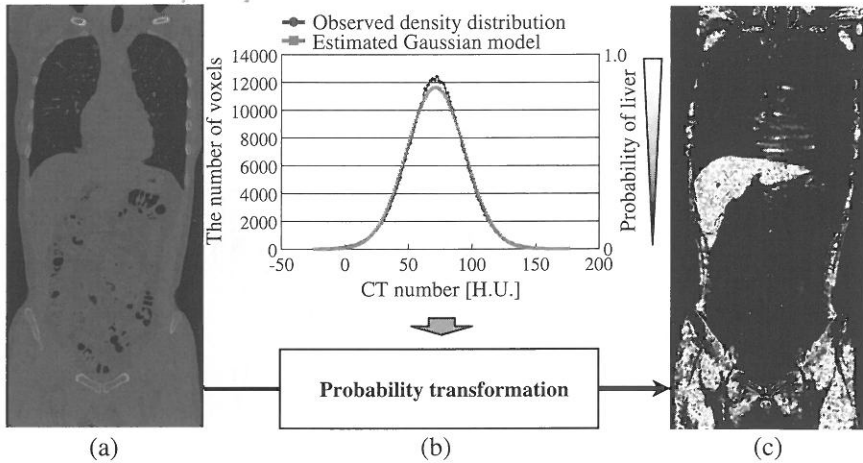
Fig. 2. The probability estimation for liver density. (a) Original CT image (1 coronal slice). (b) Probability transformation based on Gaussian model. (c) Likelihood image that shows the probability of liver on CT numbers (1 coronal slice).

from inputted CT images (Fig. 3(a)) (refer to Section 2.2). (4) Probabilistic atlas $P(A)$ (Fig. 3(f)) of liver for inputted CT images is generated by multiplication of $P(B)$ (Fig. 3(d)) and $P(C|B)$ (Fig. 3(e)). (5) The liver region is segmented by a thresholding on probabilistic atlas $P(A)$ and finally refined using a connected component processing (Fig. 3(h)). The procedure was designed in a fully-automatic mode without any assistance by operators.

## 3. Experiment and results

80 patient cases of non-contrast torso CT images were used in the experiment. Each image has an isotopic spatial resolution of about 0.6 mm and density (CT number) resolution of 12 bits. The liver region in each image was extracted for atlas construction and accuracy evaluation for segmentation results using a semi-automatic segmentation method. We evaluated the performance of our method using a leave-one-out method (selecting 79 patient cases to construct a liver atlas and use it to segment the liver region from the surplus 1 case). We also investigated the validity of our atlas construction method.

At first, we investigated the density distribution of the pre-segmented liver region in CT images and found that density histogram of liver region in each patient case was quite close to a Gaussian distribution. However, the mean value and standard deviation of the liver density in each case varied largely. Using our Gaussian parameter estimation, we confirmed that the mean coincidence ratio between the real density distribution and estimated Gaussian model was 94% in 80 patient cases. The margin of the error was caused by the vessels that were recognized incorrectly as a part of liver region during the pre-segment process. The experiential result showed that the density of liver region can be presented by a Gaussian distribution and Gaussian parameters should be estimated respectively from the CT images for the different patient cases.

We confirmed that normalizing the liver location in different patient cases was very important before constructing the probability of liver location; we compared the results of the likelihood images of liver location before the normalization (Fig. 4(a)) and after the
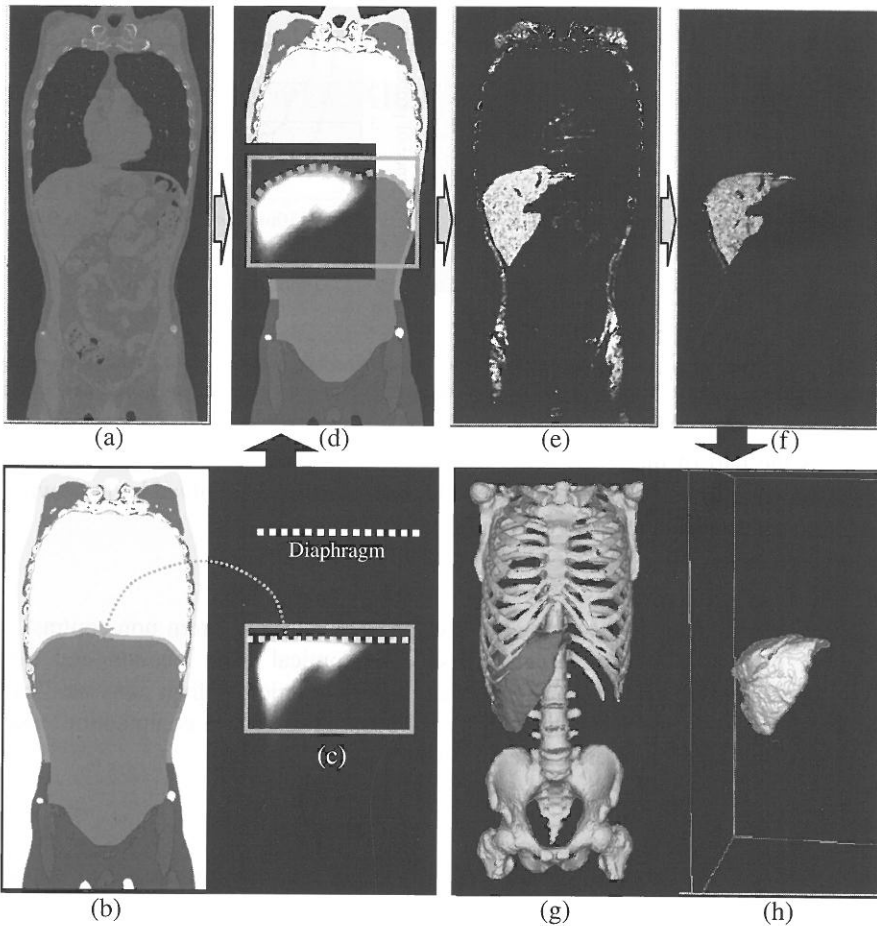
Fig. 3. The processing results of liver segmentation. (a) Original CT image. (b) Extraction results of diaphragm and bone. (c) Normalized likelihood image of liver location. (d) Likelihood image of liver location for panel (a). (e) Likelihood image of liver density. (f) Probabilistic atlas of liver region. (g) Pre-segmented liver and bone. (h) Atlas-based segmentation result of liver region.

normalization (Fig. 4(c)). We measured the convergence of probability of liver location (refer to Fig. 4(b)) and confirmed that our method (warping the diaphragm and bone structure to reduce the variance of liver location and shape in different CT images) was very effective to improve the accuracy of the atlas on liver location.

Based on the probabilistic atlas $P(A)$ (Fig. 3(f)), the liver region was extracted by simply selecting the voxel $i$ that satisfied the condition ($P_i(A) > 0.03$), and then, the binary regions were refined by a binary morphological processing [ball with $r = 2$ (pixels)]. At last, the biggest connected component was decided as the liver region. We confirmed that the liver region in each patient case was segmented correctly. The mean coincidence ratio between extracted liver region (Fig. 3(h)) and pre-segmented liver region (Fig. 3(g)) for all patient cases was about 84%. We found that this error was caused by the vessels inside of the pre-segmented liver region which has the different density distribution and was not
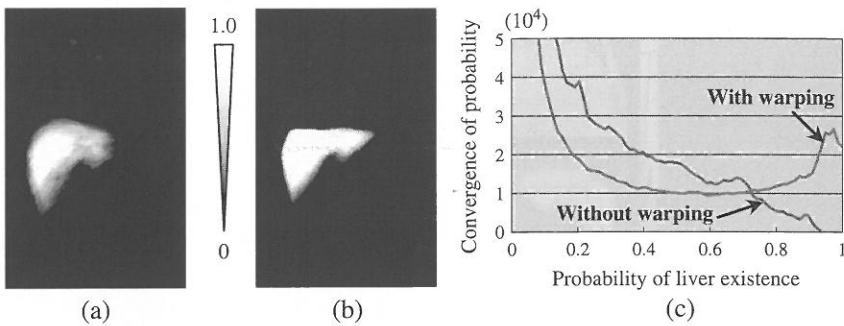
Fig. 4. The comparison of the likelihood image of liver location estimations. (a) Result without liver location normalization by warping the diaphragm. (b) Result after normalizing the liver location by diaphragm warping. (c) Convergence of the probability of liver existence with and without warping.

regarded as the part of the liver region during the atlas generation [refer to Section 2.2: $P(C|B)$ estimation using a Gaussian model]. This problem can be solved by improving the accuracy of the pre-segmented liver region.

## 4. Conclusion

We proposed a method to construct a liver probabilistic atlas from non-contrast torso CT images by estimating the probabilities of anatomical liver location and density distribution of liver region. We confirmed that our construction of liver atlas was feasible and effective; the liver probabilistic atlas may be useful to reduce computation cost and increase the robustness of liver segmentation process.

## Acknowledgements

## References

[1] H. Park, P.H. Bland, C.R. Meyer, Construction of an abdominal probabilistic atlas and its application in segmentation, IEEE Trans. Med. Imag. 22 (4) (2003) 483–492.
[2] T. Kitagawa, et al., Automated segmentation of liver region from multi-slice torso CT images based on statistical models, 90th Scientific Assembly and Annual Meeting of the Radiological Society of North America, 2004, p. 9405 (IMA-i).
[3] H. Kobatake, et al., Simultaneous segmentation of multiple organs in multi-dimensional medical images, Proc. of the First International Symposium on Intelligent Assistance in Diagnosis of Multi-dimensional Medical Images: Part I. 2005, pp. 11–18.
[4] F.L. Bookstein, Principal warps: thin-plate splines and the decomposition of deformations, IEEE Trans. PAMI 11 (6) (1989) 567–585.
[5] X. Zhou, et al., Automated segmentations of skin, soft-tissue and skeleton from torso CT images, Proc. SPIE-Med. Imaging 5370 (2004) 1634–1639.
[6] X. Zhou, et al., Automated extraction and recognition of anatomical body cavity from multi-slice torso CT images, Proc. of 19th International Congress of CARS—Computer Assisted Radiology and Surgery, 2005.